Deconfined SU(2) phase with a massive vector boson triplet

Bernd A. Berg
Department of Physics, Florida State University, Tallahassee, FL 32306-4350, USA
(Dated: December 1, 2010)

We introduce a model of SU(2) and U(1) vector fields with a local U(2) symmetry. Its action can be obtained in the London limit of a gauge invariant regularization involving two scalar fields. Evidence from lattice simulations of the model supports a (zero temperature) SU(2) deconfining phase transition through breaking of the SU(2) center symmetry, and a massive vector boson triplet is found in the deconfined phase.

PACS numbers: 11.15.Ha, 12.15.-y, 12.60.Cn, 12.60.-i, 14.80.Bn

I. INTRODUCTION

Euclidean field theory notation is used throughout this paper. The action of the electroweak gauge part of the standard model reads

$$S = \int d^4x\, L^{\rm ew}\,, \tag{1}$$

$$L^{\rm ew} = -\frac{1}{4}\, F^{\rm em}_{\mu\nu} F^{\rm em}_{\mu\nu} - \frac{1}{2}\,{\rm Tr}\, F^b_{\mu\nu} F^b_{\mu\nu}\,, \tag{2}$$

$$F^{\rm em}_{\mu\nu} = \partial_\mu a_\nu - \partial_\nu a_\mu\,, \tag{3}$$

$$F^b_{\mu\nu} = \partial_\mu B_\nu - \partial_\nu B_\mu + i g_b\,[B_\mu, B_\nu]\,, \tag{4}$$

where a'_μ are U(1) and B_μ are SU(2) gauge fields.

Typical textbook introductions of the standard model, e.g. [1], emphasize at this point that the theory contains four massless gauge bosons and introduce the Higgs mechanism so that one obtains a massive vector boson triplet and only one gauge boson, the photon, stays massless. Such presentations reflect that the introduction of the Higgs particle in electroweak interactions [2] preceded our non-perturbative understanding of non-Abelian gauge theories.

In fact, massless gluons are not in the physical spectrum of (1). The self interaction due to the commutator (4) generates dynamically a non-perturbative mass gap, and the SU(2) spectrum consists of massive glueballs. The lightest glueball can be used to set a mass scale. Choosing for it, e.g., 80 GeV and coupling fermions is perfectly admissible. This does not constitute an ansatz for an electroweak theory by two reasons: The SU(2) glueball spectrum is not what is wanted (e.g., masses of spin 0 and 2 states are lower than for spin 1 [3]) and fermions would be confined into boundstates, which is not the case. Coupling a Higgs field causes a deconfining phase transition, so that fermions are liberated, a photon stays massless and glueballs break up into elementary massive vector bosons. Such a confinement-Higgs transition has indeed been observed in pioneering lattice gauge theory (LGT) investigations [4]. The present paper introduces a different model for which a zero-temperature deconfined phase breaks the Z_2 center symmetry of SU(2) and exhibits a massive vector boson triplet.

The motivation for the action defined in the next section comes from properties of the U(1) Polyakov loop.

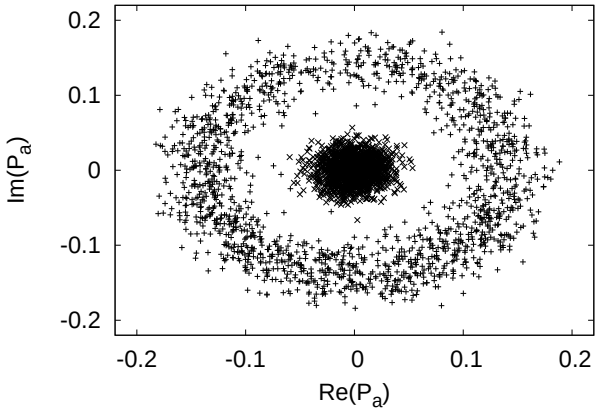

FIG. 1: Scatter plot for U(1) Polyakov loops on a 12^4 lattice at $\beta_a = 0.9$ in the symmetric phase (center) and at $\beta_a = 1.1$ in the broken phase (ring).

U(1) LGT confines fermions in the strong coupling limit of its lattice regularization [5]. At weaker coupling it undergoes a transition into the Coulomb phase as has been rigorously proven [6]. In the Coulomb phase the effective potential of the U(1) Polyakov loop P_a assumes the Mexican hat shape that is also characteristic for a complex Higgs field in the broken phase. This is illustrated in Fig. 1 by scatter plots of Polyakov loops in the symmetric and in the broken phase. From the ring-like distribution in the broken phase the similarity with the behavior of a Higgs field is evident (details of the simulations for the figure are given in section III).

We introduce a contribution to the action that is the alternating product of SU(2) and U(1) gauge matrices around a plaquette. It unifies SU(2) and U(1) gauge transformations into a local U(2) symmetry, which we take as the starting point of our presentation in section II. A gauge invariant regularization is obtained by coupling two scalar fields [7] and leads to our model by freezing these fields up to their gauge transformations, here called London [8] limit. The scalar fields can then be absorbed by extended gauge transformations, which were introduced and discussed in [9, 10]. Some technical details of section II encountered in the investigation of

the classical continuum limit are relegated to appendixes.

In section III we investigate the quantum field theory numerically in the lattice regularization. Evidence for a SU(2) deconfining phase transition, first observed in [9], and results for the particle spectrum are presented. A massless photon is found in both phases. Noisy correlations (as usual) indicate massive SU(2) glueballs, which appear to jump to unphysically high mass values in the deconfined phase. A beautiful strong signal for correlation functions of a massive vector boson triplet is seen in the deconfined phase, while it does not exist on the confined side.

Summary, outlook and conclusions follow in the final section IV.

II. ACTION AND GAUGE TRANSFORMATIONS

Introducing gauge fields is often motivated by promoting a global symmetry of matter fields to a local one. Let us assume a global U(2) symmetry:

$$\psi \;\to\; \psi\,' = G\,\psi \;\text{ with }\; G = G_1 G_2\,, \qquad G_1 \in U(1) \;\text{ and }\; G_2 \in SU(2)\,. \tag{5}$$

The $\overline{\psi}\gamma_\mu\partial_\mu\psi$ part of the free fermion Lagrangian breaks (5) as a local symmetry. This is overcome by coupling to gauge fields, whose transformation behavior cancels the unwanted contributions out. In the lattice regularization the relevant coupling reads

$$a^3 K_\mu\, \overline{\psi}(na)\, U_\mu(na) V_\mu(na) \psi(na+\hat{\mu}a)\,, \tag{6}$$

where $n = (n_1, n_2, n_3, n_4)$ is a vector of integers, $\hat{\mu}$ is the unit vector in μ direction, a the lattice spacing ($x = na$),

$$U_\mu = e^{ig_a a A_\mu} \in U(1) \text{ and } V_\mu = e^{ig_b a B_\mu} \in SU(2)\,. \tag{7}$$

Here g_a and g_b are introduced as U(1) and SU(2) coupling constants. The precise definition of the fermions (see for instance [11, 12]) in Eq. (6) is accomplished by K_μ and irrelevant in our context as we discuss only their gauge transformations. The classical continuum limit is for $a \to 0$ obtained from a^4 contributions, whose sum becomes an integration over space.

In the lattice formulation it is obvious that the local gauge transformations

$$\psi(na) \;\to\; G(na)\,\psi(na) = G_1(na)\,G_2(na)\,\psi(na) \tag{8}$$

will be absorbed by imposing the transformations

$$U_\mu(na) \;\to\; G_1(na) U_\mu(na) G_1^{-1}(na+\hat{\mu}a)\,, \tag{9}$$

$$V_\mu(na) \;\to\; G_2(na) V_\mu(na) G_2^{-1}(na+\hat{\mu}a)\,, \tag{10}$$

on the vector fields, provided that their contributions to the action are gauge invariant. This is (for instance) fulfilled for the Wilson action

$$S^{\text{gauge}} = \frac{\beta_a}{2}\sum_p \text{Re}\,\text{Tr}\,U_p + \frac{\beta_b}{2}\sum_p \text{Tr}\,V_p \tag{11}$$

where the sums are over all plaquettes and U_p, V_p are oriented products of gauge matrices around the plaquette loop. E.g., for a V_p plaquette in the $\mu\nu$, $\mu \neq \nu$ plane:

$$V_{\mu\nu}(x) = \text{Tr}\,\left[V_\mu(x)\,V_\nu(x+\hat{\mu}a)\,V_\mu^\dagger(x+\hat{\nu}a)\,V_\nu^\dagger(x)\right]\,.$$

As it turns out to be convenient, we represent here and in the following U(1) phase factors by diagonal 2×2 matrices with a_μ (1) and A_μ (7) related by

$$A_\mu = \frac{1}{2}\,\tau_0\,a_\mu\,, \tag{12}$$

where τ_0 is the 2×2 unit matrix. The electromagnetic contribution to the Lagrangian (1) reads then

$$L^a \;=\; -\frac{1}{2}\,\text{Tr}\,F^a_{\mu\nu}F^a_{\mu\nu}\,,\quad F^a_{\mu\nu} \;=\; \partial_\mu A_\nu - \partial_\nu A_\mu\,. \tag{13}$$

The equations

$$\beta_a = \frac{1}{g_a^2} \;\text{ and }\; \beta_b = \frac{4}{g_b^2}\,. \tag{14}$$

relate β_a and β_b of (11) to the couplings g_a and g_b of (7). More lattice actions that give the classical continuum limit (1) are discussed in [13].

There is an asymmetry in the way the gauge transformations work: A transformation of either the U(1) or the SU(2) matrices implies the corresponding transformation for the fermion field, while there is no such effect on the other gauge field. Another remarkable [14] feature of the action (11) is that it is additive and not multiplicative in the U(1) and SU(2) fields. Changing also the fermion terms (6) to additive

$$a^3 K_\mu\, \overline{\psi}(na)\, U_\mu(na) \psi(na+\hat{\mu}a) \tag{15}$$

$$+\;\; a^3 K_\mu\, \overline{\psi}(na)\, V_\mu(na) \psi(na+\hat{\mu}a)\,, \tag{16}$$

the a^4 contributions to the classical $a \to 0$ limit remain unchanged, while the gauge transformations become symmetrical in all fields, because Eq. (9) and (10) have to be replaced by local U(2) transformations

$$U_\mu(na) \;\to\; G(na) U_\mu(na) G^{-1}(na+\hat{\mu}a)\,, \tag{17}$$

$$V_\mu(na) \;\to\; G(na) V_\mu(na) G^{-1}(na+\hat{\mu}a)\,, \tag{18}$$

which we call *extended gauge transformations* while reserving the notation *gauge transformations* for their conventional version.

The gauge part (11) of the action is invariant under local U(2) transformations. After a generic transformation former U(1) and SU(2) matrices will both be in U(2) and their identification as U(1) or SU(2) has become converted into constraints on the gauge manifold. The special gauge in which they are actually in U(1) and SU(2), i.e. Eq. (7) holds, will be called *diagonal gauge*. In this gauge the U(1) part is not only diagonal but proportional to the unit matrix. With reference to the existence of this gauge we keep the U(1) and SU(2) matrix identifications.

Requiring invariance only under extended gauge transformations (17) and (18) allows for new additions to the action. Numerically we investigate

$$S^{\rm add} \;=\; \sum_{\mu\nu} S^{\rm add}_{\mu\nu}\,, \quad S^{\rm add}_{\mu\nu} \;= \tag{19}$$

$$\frac{\lambda}{2}\,{\rm Re\,Tr}\,\left[U_\mu(x)\,V_\nu(x+\hat{\mu}a)\,U^\dagger_\mu(x+\hat{\nu}a)\,V^\dagger_\nu(x)\right]\,. \tag{20}$$

A gauge invariant regularization is [7]

$$S^s \;=\; \sum_x \left\{ \sum_{\mu\nu} S^s_{\mu\nu} + \kappa\,{\rm Tr}\,\left[\left(\Phi^\dagger\,\Phi - \tau_0\right)^2\right]\right\}, \tag{21}$$

$$\begin{aligned} S^s_{\mu\nu} \;=\; & \frac{\lambda^s}{4}{\rm Re\,Tr}\,\{U_\mu(x)U^\dagger_\mu(x+\hat{\nu}a) \\ & [\Phi^\dagger(x+\hat{\mu}a)\,V_\nu(x+\hat{\mu}a)\,\Phi(x+\hat{\mu}a+\hat{\nu}a)] \\ & [\Phi^\dagger(x)\,V_\nu(x)\,\Phi(x+\hat{\nu}a)]^\dagger\} \end{aligned} \tag{22}$$

where Φ is a 2×2 matrix scalar field that is charged with respect to $U(1)$ and $SU(2)$. Its gauge transformations are

$$\Phi \;\to\; e^{-i\alpha}\,g\,\Phi\,, \tag{23}$$

where $g\in$ SU(2), $e^{i\alpha}\in$ U(1). In the London [8] limit $\kappa\to\infty$ this action is equivalent to (19), because Φ takes on it vacuum value, which is a pure gauge

$$\Phi \;=\; e^{-i\alpha}\,g\,. \tag{24}$$

Fixing the gauge to $\Phi=\tau_0$ yields (19) and on finite lattices properties at sufficiently large κ values are expected to be practically identical.

It is only in the limit $\kappa\to\infty$ that the coupling constant λ^s together with the dimensions of the scalar fields becomes the dimensionless coupling λ of (19) (recall that the dimensionless lattice field Φ is related to the physical scalar field $\Phi_{\rm phys}$ by $\Phi = a\,\Phi_{\rm phys}$ [12]). This is opposite to what happens in the SU(2) Higgs model where the interaction between scalar field and SU(2) field, as for instance given in [15], is proportional to

$$\lambda^s_h \sum_x \sum_{\mu=1}^4 {\rm Tr}\,\left(\phi^\dagger_{x+\hat{\mu}a}\,V_\mu(x)\,\phi_x\right)\,, \tag{25}$$

with $\phi=\rho\,g$, $\rho>0$, $g\in$ SU(2). Here λ^s_h is dimensionless, and fixing the gauge in the London limit to $\phi=\tau_0$ leads to the gauge symmetry breaking contribution

$$\lambda_h \sum_x \sum_{\mu=1}^4 {\rm Tr}\,V_\mu(x)\,, \tag{26}$$

where λ_h acquires the dimension of the $\phi^\dagger\phi$ scalar fields.

The extended gauge transformations (17) and (18) restore the transformation (23) without using scalar fields by absorbing the $\exp(-i\alpha)$ phase factor into the V_μ and the SU(2) transformation g into the U_μ field. This requires the action (19), or similar, and is not possible in the London limit (26) of the Higgs model.

Before investigating the quantum field theory (19) numerically, we consider the classical continuum limits of (19) and (21).

A. Classical continuum limit

The classical Lagrangian is expected to be the effective theory at energy scales much larger than the masses of the model. In the limit $a\to 0$ the a^4 contributions of (20) give

$$L^{\rm add} \;=\; -\frac{\lambda}{4}\,{\rm Tr}\left(F^{\rm add}_{\mu\nu}F^{\rm add}_{\mu\nu}\right)\,, \tag{27}$$

$$F^{\rm add}_{\mu\nu} \;=\; g_b\partial_\mu B_\nu - g_a\partial_\nu A_\mu + i\,g_a g_b\,[A_\mu,B_\nu]\,, \tag{28}$$

where the commutator reflects that B_μ and A_ν will in general not commutate unless we are in the diagonal gauge, defined in-between Eq. (18) and (19).

Let us translate the extended gauge transformations (17) and (18) into continuum notation. Consider the gauge-covariant derivative

$$D^{\rm em}_\mu = \partial_\mu + ig_a a_\mu \tag{29}$$

of an electromagnetic field $a_\mu(x)$ on a complex fermion field $\psi(x)$. With the gauge transformations

$$\psi \;\to\; \psi' = e^{i\alpha(x)}\,\psi\,, \tag{30}$$

$$a_\mu(x) \;\to\; a'_\mu = a_\mu - \frac{i}{g_a}\,\partial_\mu\alpha(x) \tag{31}$$

one finds

$$D^{\rm em}_\mu\psi \to D^{'{\rm em}}_\mu\psi' = e^{i\alpha(x)}D^{\rm em}_\mu\psi\,, \tag{32}$$

so that the Lagrangian

$$L^{\rm em}_\psi = \overline{\psi}\left(i\gamma_\mu D^{em}_\mu - m\right)\psi - \frac{1}{4}F^{\rm em}_{\mu\nu}F^{\rm em}_{\mu\nu} \tag{33}$$

is gauge invariant, where

$$F^{\rm em}_{\mu\nu} = \frac{1}{ig_a}\left[D^{em}_\mu, D^{em}_\nu\right]\,. \tag{34}$$

is the field tensor.

Assume now that $\psi(x)$ is a complex doublet, which transforms under local U(2) transformations

$$\psi \;\to\; \psi' = G(x)\,\psi\,, \tag{35}$$

$$G(x) \;=\; \exp\left(\frac{i}{2}\sum_{i=0}^3 \tau_i\alpha_i(x)\right)\,. \tag{36}$$

Here τ_0 is as in (12) the 2×2 unit matrix and τ_i, $i=1,2,3$ are the Pauli matrices. We still can couple ψ in an

invariant way to an electromagnetic field. We define the gauge covariant derivative by

$$D^a_\mu = \partial_\mu + ig_a A_\mu \tag{37}$$

and the extended gauge transformations of A_μ by (compare for instance Ref. [1] for usual SU(2) gauge transformations)

$$A_\mu \to A'_\mu = GA_\mu G^{-1} + \frac{i}{g_a}(\partial_\mu G)\, G^{-1} \tag{38}$$

which adds to the U(1) field the transformation of a null SU(2) field and yields the desired result

$$D^a_\mu \psi \to D^{'a}_\mu \psi' = G D^a_\mu \psi\,. \tag{39}$$

The field tensor defined by

$$F^a_{\mu\nu} = \frac{1}{ig_a}\left[D^a_\mu, D^a_\nu\right] \tag{40}$$

transforms as

$$F^a_{\mu\nu} \to F^{'a}_{\mu\nu} = G F^a_{\mu\nu} G^{-1} \tag{41}$$

so that the Lagrangian

$$L^a_\psi = \overline{\psi}\left(i\gamma_\mu D^a_\mu - m\right)\psi - \frac{1}{2}\mathrm{Tr}\left(F^a_{\mu\nu}F^a_{\mu\nu}\right) \tag{42}$$

stays invariant. The local U(2) transformations do not destroy the fact that A_μ describes just an electromagnetic field. Any $A_\mu(x)$ field is gauge equivalent to one in the diagonal gauge for which A_μ is proportional to the unit matrix. Consequently, $F^{'a}_{\mu\nu}$ stays always diagonal and the G matrices can be omitted in (41).

Similarly, we extend gauge transformations of a SU(2) field $B_\mu(x)$ by a phase. The gauge covariant derivative is

$$D^b_\mu = \partial_\mu + ig_b B_\mu \quad \text{with} \quad B_\mu = \frac{1}{2}\,\vec{\tau}\cdot\vec{b}_\mu \tag{43}$$

and the extended gauge transformations of B_μ are

$$B_\mu \to B'_\mu = GB_\mu G^{-1} + \frac{i}{g_b}(\partial_\mu G)\, G^{-1}\,. \tag{44}$$

Equations (39) to (42) carry simply over by replacing all labels a by b.

An electroweak Lagrangian of the type

$$\begin{aligned} L^{ab}_\psi \;&=\; -\frac{1}{2}\mathrm{Tr}\left(F^a_{\mu\nu}F^a_{\mu\nu}\right) - \frac{1}{2}\mathrm{Tr}\left(F^b_{\mu\nu}F^b_{\mu\nu}\right) \\ &+\; \overline{\psi}\left(i\gamma_\mu D^a_\mu - m\right)\psi + \overline{\psi}\left(i\gamma_\mu D^b_\mu - m\right)\psi \end{aligned} \tag{45}$$

allows one to add (27). Under extended gauge transformations (38) for A_μ and (44) for B_μ, the $F^{\mathrm{add}}_{\mu\nu}$ tensor (28) transforms according to

$$F^{\mathrm{add}}_{\mu\nu} \to F^{'\mathrm{add}}_{\mu\nu} = G\, F^{\mathrm{add}}_{\mu\nu}\, G^{-1}\,, \tag{46}$$

so that L^{add} is invariant. The algebra for (46) is given in appendix A.

As it is tedious and not very enlightening to calculate the classical continuum limit of the action (21) with scalar fields, we relegate its discussion to appendix B. The essence is caught by a much simpler gauge invariant classical interaction with two scalar fields, which reduces also to (27) in the London limit, but has a lattice regularization that differs from (21).

Let us introduce the scalar fields

$$\phi_1 = \rho\, e^{i\alpha}\,\tau_0,\ \rho > 0 \ \text{ and } \ \phi_2 = \sigma\, g,\ \sigma > 0 \tag{47}$$

with $g \in \mathrm{SU}(2)$. It is then easy algebra to show that the field tensor

$$\begin{aligned} S^s_{\mu\nu} \;&=\; \phi_2^\dagger\, D^b_\mu\, D^b_\nu\, \phi_2 + (D^b_\mu\,\phi_2)^\dagger\, D^b_\nu\,\phi_2 \\ &-\; \phi_1^\dagger\, D^a_\nu\, D^a_\mu\, \phi_1 - (D^a_\nu\,\phi_1)^\dagger\, D^a_\mu\,\phi_1 \end{aligned} \tag{48}$$

reduces by gauge fixing in the London limit to $i\,F^{\mathrm{add}}_{\mu\nu}$ (28) in the diagonal gauge, so that

$$L^s = -\frac{\lambda}{4}\,\mathrm{Tr}\,\left[\left(S^s_{\mu\nu}\right)^\dagger\ S^s_{\mu\nu}\right] \tag{49}$$

becomes a gauge invariant extension of (27).

III. NUMERICAL INVESTIGATION

Pure U(1) LGT with the Wilson action has at $\beta_a \approx 1.01$ a phase transition from its confined into its Coulomb phase. Presumably the transition is weakly first order as first reported in [16]. We have calculated lattice averages of U(1) Polyakov loops P_a by Monte Carlo (MC) simulations on a 12^4 lattice with periodic boundary conditions with a statistics of 10,000 sweeps for equilibration and 160,000 sweeps with measurements. Measurements are plotted every 20 sweeps. Figure 1 compares scatter plots at $\beta_a = 0.9$ in the disordered confined phase and at $\beta_a = 1.1$ in the ordered Coulomb phase. In the unbroken disordered phase the values scatter about zero, while they form a ring in the broken ordered phase. As the transition happens at zero temperature, this holds on a symmetric lattice for Polyakov loops winding in any one of the four directions through the torus (ordered starts are used to avoid metastabilities of the MC algorithm).

In the following MC simulations with the plaquette action

$$S \;=\; S^{\mathrm{gauge}} + S^{\mathrm{add}} \tag{50}$$

are performed, where S^{gauge} is defined by (11) and S^{add} by (19). We use lattice units $a = 1$ in this section.

A. Integration measure and Monte Carlo updating

Our MC procedure proposes the usual U(1) and SU(2) changes. For the update of a U(1) matrix $U_\mu(n)$ we need

the contribution to (50), which comes from the eight staples containing this matrix

$$\begin{aligned} U_{\sqcup,\mu}(n) &= \frac{\beta_a}{2}\sum_{\nu\neq\mu}\big[U_\nu(n+\hat\mu)\,U_\mu^\dagger(n+\hat\nu)\,U_\nu^\dagger(n) \\ &+ U_\nu^\dagger(n+\hat\mu-\hat\nu)\,U_\mu^\dagger(n-\hat\nu)\,U_\nu(n-\hat\nu)\big] \\ &+ \frac{\lambda}{2}\sum_{\nu}\big[V_\nu(n+\hat\mu)\,U_\mu^\dagger(n+\hat\nu)\,V_\nu^\dagger(a) \\ &+ V_\nu^\dagger(n+\hat\mu-\hat\nu)\,U_\mu^\dagger(n-\hat\nu)\,V_\nu(n-\hat\nu)\big] \quad (51) \end{aligned}$$

and correspondingly for the SU(2) matrix $V_\mu(n)$

$$\begin{aligned} V_{\sqcup,\mu}(n) &= \frac{\beta_b}{2}\sum_{\nu\neq\mu}\big[V_\nu(n+\hat\mu)\,V_\mu^\dagger(n+\hat\nu)\,V_\nu^\dagger(n) \\ &+ V_\nu^\dagger(n+\hat\mu-\hat\nu)\,V_\mu^\dagger(n-\hat\nu)\,V_\nu(n-\hat\nu)\big] \\ &+ \frac{\lambda}{2}\sum_{\nu}\big[U_\nu(n+\hat\mu)\,V_\mu^\dagger(n+\hat\nu)\,U_\nu^\dagger(n) \\ &+ U_\nu^\dagger(n+\hat\mu-\hat\nu)\,V_\mu^\dagger(n-\hat\nu)\,U_\nu(n-\hat\nu)\big]\ . \quad (52) \end{aligned}$$

Updates are then performed with the Gibbs-Boltzmann weights

$$dU_\mu(n)\ \ \exp\{\,\mathrm{ReTr}\,[U_\mu(n)\,U_{\sqcup,\mu}(n)]\,\}\ , \quad (53)$$
$$dV_\mu(n)\ \ \exp\{\,\mathrm{ReTr}\,[V_\mu(n)\,V_{\sqcup,\mu}(n)]\,\}\ . \quad (54)$$

where the $dU_\mu(n)$ integration is from $-\pi$ to $+\pi$ over the phase $\phi_\mu(n)$ of the matrix $U_\mu(n)=\exp[i\,\phi_\mu(n)]$ and $dV_\mu(n)$ is over the SU(2) Hurwitz [17] measure. This is well suited and done with the biased Metropolis-heatbath algorithm [18].

It is instructive to discuss (54) for the case in which the U(1) matrices in (52) are aligned as it is approximately the case in the U(1) Coulomb phase. Then the U(1) matrices cancel out, so that large values of λ favor $\mathrm{Tr}[V_\mu(n)V_\mu^\dagger(n+\hat\nu)]=\mathrm{Tr}[V_\mu(n)V_\mu^\dagger(n-\hat\nu)]=2$ and, hence, the SU(2) matrices are also aligned, $V_\mu(n)=V_\mu(n+\hat\nu)=V_\mu(n-\hat\nu)$. SU(2) deconfinement (breaking of the Z_2 center group) is achieved when this effect (spoiled by U(1) fluctuations at finite λ) becomes strong enough. Integrations with the measures (53) and (54) do not include extended gauge transformations (17) and (18). Updates stay within the diagonal gauge defined in section II. Within the MC procedure only global SU(2) transformations $V_\mu(n)\to GV_\mu(n)G^{-1}$ with the same G for all SU(2) matrices remain.

The partition function of the MC calculation

$$Z\{G(n)\} \;=\; \int\prod_n\prod_{\mu=1}^{4} dU_\mu(n)\,dV_\mu(n)\,e^{S\{U_\mu(n),V_\mu(n)\}} \quad (55)$$

is invariant under extended $U(2)$ gauge transformation (17) and (18). The Jacobian determinants of both $\prod_n\prod_\mu dU_\mu(n)$ and $\prod_n\prod_\mu dV_\mu(n)$ are one and the action (50) is by construction invariant. U(1) and SU(2) Wilson loops are invariant operators as the U(2) transformations drop out in the trace. As usual [11, 12] their physical interpretation can be derived by imagining a coupling to static quarks. In addition to the normal Wilson loops traces of corresponding mixed products of U(1) and SU(2) matrices are also invariant, but we make no use of them in the following.

With normalization of the integration over the $U(2)$ measure to one, the identity

$$Z \;=\; \int\prod_n dG(n)\,Z\{G(n)\} \;=\; Z\{G(n)\} \quad (56)$$

holds under extended gauge transformations. This integration can easily be added to the updates: At site n all matrices on links emerging at n will be transformed according to

$$U_\mu(n)\to G(n)\,U_\mu(n)\,,\quad V_\mu(n)\to G(n)\,V_\mu(n) \quad (57)$$

and all matrices on links ending at n according to

$$\begin{aligned} U_\mu(n-\hat\mu) &\to U_\mu(n-\hat\mu)\,G^{-1}(n)\,, \\ V_\mu(n-\hat\mu) &\to V_\mu(n-\hat\mu)\,G^{-1}(n)\,. \quad (58) \end{aligned}$$

The acceptance rate of such updates is 100% as no change in the value of the action is implied.

The unusual feature is that the integration measure of the vector fields $U_\mu(n)$ and $V_\nu(n)$ in the functional integral (55) is not identical with the gauge measures in (56). However, for gauge transformations of scalar and fermion fields we are used to this and there appears no strong argument against having a distinction of these measures also for vector fields (calling them gauge fields may have added to the expectation that functional and gauge measures are the same).

B. Zero temperature SU(2) deconfining transition

We keep the U(1) coupling at $\beta_a=1.1$ and for the SU(2) coupling the values $\beta_b=2.3$ is used. At $\lambda=0$, without interaction, β_a is in the U(1) Coulomb phase and β_b in the SU(2) scaling region. Runs are performed on 12^4 lattices. Data points are based on a statistics of at least 2^{10} sweeps without measurements and subsequently 32×2^{10} sweeps with measurements. Error bars are calculated with respect to the 32 blocks.

With increasing λ one finds a strong first order phase transition, which is illustrated in Fig. 2 for the expectation values of the various plaquette actions. From up to down: $\langle\mathrm{ReTr}U_p\rangle/2$ for U(1), $\langle\mathrm{Tr}V_p\rangle/2$ for SU(2) both contributing to (11) and $\lambda^{-1}\sum_{\mu\nu}\langle S_{\mu\nu}^{\mathrm{add}}\rangle/16$ for Mixed (19), which drives the transition. Disordered starts are marked by "d" and ordered starts by "o". The values are compiled in table I.

Creutz ratios [20] for the SU(2) and U(1) string tensions are calculated from Wilson loops up to size 5×5. Fig. 3 shows for $\beta_b=2.3$ the behavior of the square roots

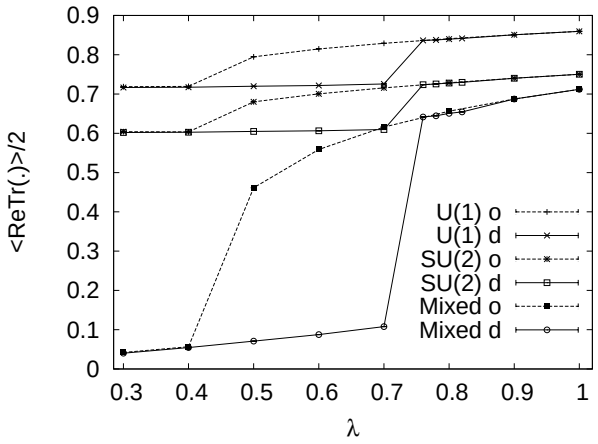

FIG. 2: Plaquette expectation values on a 12^4 lattice as function of λ with $\beta_a = 1.1$ and $\beta_b = 2.3$ (ordered o and disordered d starts).

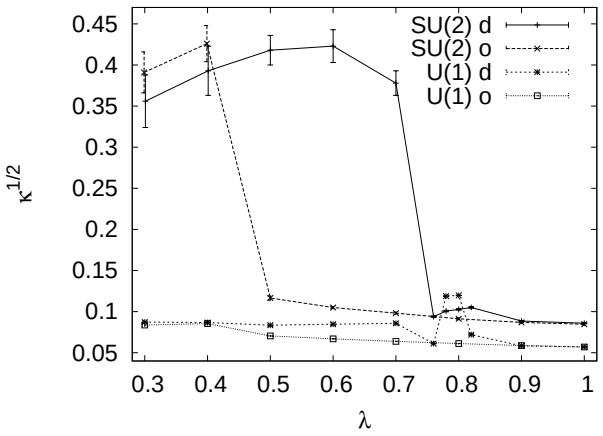

FIG. 3: SU(2) and U(1) string tensions from Creutz ratios on a 12^4 lattice as function of λ with $\beta_a = 1.1$ and $\beta_b = 2.3$ (disordered d and ordered o starts).

TABLE I: Plaquette expectation values of Fig. 2.

λ	U(1)	SU(2)	Mixed
0.30 d	0.716576 (17)	0.601961 (29)	0.040142 (08)
0.40 d	0.717373 (17)	0.602630 (27)	0.054590 (08)
0.50 d	0.719702 (21)	0.604709 (21)	0.070845 (08)
0.60 d	0.721775 (19)	0.606398 (22)	0.087592 (10)
0.70 d	0.725563 (21)	0.609602 (29)	0.107814 (21)
0.76 d	0.836426 (08)	0.723714 (08)	0.641590 (14)
0.78 d	0.837722 (08)	0.725532 (09)	0.644591 (14)
0.80 d	0.839750 (07)	0.727838 (09)	0.650849 (10)
0.82 d	0.841460 (34)	0.729742 (11)	0.654499 (56)
0.90 d	0.850887 (07)	0.740039 (07)	0.687311 (11)
1.00 d	0.859572 (07)	0.750205 (08)	0.712059 (07)
0.30 o	0.718566 (19)	0.603975 (21)	0.042148 (06)
0.40 o	0.719359 (19)	0.603618 (25)	0.056604 (09)
0.50 o	0.794571 (11)	0.680028 (10)	0.461244 (39)
0.60 o	0.814685 (11)	0.700420 (07)	0.558826 (22)
0.70 o	0.829112 (08)	0.715794 (08)	0.615873 (14)
0.80 o	0.840897 (09)	0.728681 (09)	0.656371 (15)
0.90 o	0.850874 (06)	0.740036 (08)	0.687314 (07)
1.00 o	0.859553 (08)	0.750204 (08)	0.712054 (09)

TABLE II: String tension values $\sqrt{\kappa}$ of Fig. 3.

λ	U(1) d	SU(2) d	U(1) o	SU(2) o
0.30	0.0873 (16)	0.356 (32)	0.0837 (13)	0.391 (25)
0.40	0.0868 (18)	0.393 (30)	0.0855 (16)	0.426 (22)
0.50	0.0835 (16)	0.418 (18)	0.07045 (64)	0.1166 (25)
0.60	0.0847 (17)	0.423 (20)	0.06694 (45)	0.1050 (13)
0.70	0.0858 (16)	0.378 (15)	0.06388 (40)	0.0982 (13)
0.76	0.06117 (35)	0.0940 (10)	–	–
0.78	0.11887 (21)	0.1007 (09)	–	–
0.80	0.11979 (21)	0.1027 (10)	0.06124 (33)	0.0913 (12)
0.82	0.0720 (12)	0.1051 (10)	–	–
0.90	0.05839 (32)	0.0886 (08)	0.05874 (33)	0.0869 (07)
1.00	0.05714 (28)	0.0860 (08)	0.05704 (27)	0.0847 (09)

of the string tensions in lattice units $a = 1$ as function of λ. Error bars are calculated with respect to 32 jackknife bins, following the scheme of [19]. While the jump in the plaquette actions is similar for U(1) and SU(2), this is not the case for the string tensions. For SU(2) $\sqrt{\kappa}$ decreases at the transition by a factor 3.5, whereas the drop of $\sqrt{\kappa}$ for U(1) is just 25%. The $\sqrt{\kappa}$ values are compiled in table II.

The interpretation of Fig.3 is that the U(1) string tension signals the deconfined phase on both sides of the transition, while the SU(2) string tension is characteristic for the confined phase at small λ and for a zero-temperature deconfined phase at large λ. The latter point is supported by comparison with the behavior of the U(1) string tension for $\beta_b = \lambda = 0$ at the U(1) deconfining phase transition as shown in Fig. 4. The discontinuity in the string tension is as in Fig. 3 for SU(2), only that no strong metastabilities are observed for U(1).

Polyakov loop measurements support also the SU(2) deconfining phase transition. Fig. 5 shows histograms for SU(2) Polyakov loops P_b at $\lambda = 0.4$ in the confined and at $\lambda = 0.9$ in the deconfined phase. In the confined phase the values scatter symmetrically about zero, whereas in the deconfined phase the Z_2 center symmetry is broken and the values scatter about a mean of 0.14458 (45). A very long run would produce a double peak at $\lambda = 0.9$, but our run time was far too short to overcome the free energy barrier between the two peaks. Scatter plots of the U(1) Polyakov loops at the same couplings give in good approximation the ring of Fig. 1 at $\lambda = 0.4$ and a more pronounced ring at $\lambda = 0.9$, both deconfined. This interpretation is confirmed by evidence for a massless photon on both sides and of interest because compact

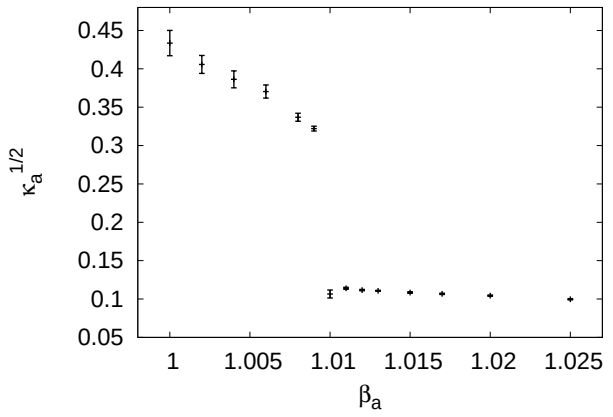

FIG. 4: U(1) string tension from Creutz ratios on a 12^4 lattice as function of β_a ($\beta_b = \lambda = 0$).

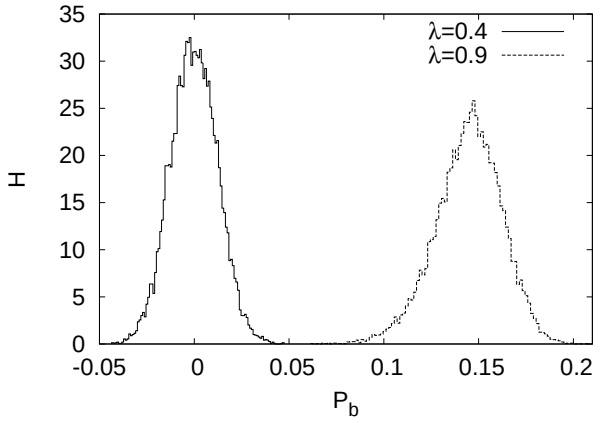

FIG. 5: Normalized SU(2) Polyakov loop histogram H at $\beta_a = 1.1$, $\beta_b = 2.3$ with $\lambda = 0.4$ (left) and $\lambda = 0.9$ (right).

U(1) LGT allows in contrast to non-compact U(1) LGT also for a confined phase.

C. Spectrum calculations

Mass spectrum calculations were performed on lattices of size N^3N_t, $N_t > N$ in the range $4^3 16$ to $12^3 64$ with a statistics of $n_{\rm eq}$ sweeps for reaching equilibrium and $32 \times n_{\rm eq}$ sweeps with measurements. Data analysis with respect to 32 bins follows again the jackknife scheme of [19]. The $n_{\rm eq}$ values used for different lattice sizes are contained in table III. All simulations reported in this section are at $\beta_a = 1.1$ and $\beta_b = 2.3$.

First, we estimate the photon mass at $\lambda = 0.4$ in the disordered SU(2) phase and in the ordered SU(2) phase at $\lambda = 0.9$. Following [21] this is done via the lattice dispersion relation (derived for a free field, for instance, in [12])

$$m^2_{\rm photon} \;=\; E^2_{k_1} - 4\,\sin^2\left(\frac{k_1}{2}\right) \qquad (59)$$

where E_{k_1} is the energy of the U(1) momentum eigenstate $(k_1, 0, 0)$, $k_1 = 2\pi/N$, of the plaquette trial operator in the T_1^{+-} representation of the cubic group. Energies are estimated from correlation functions $c(t)$ of operators by the usual two parameter (a_1 and E) cosh fits

$$c(t) \;=\; a_1\,\left(e^{-E\,t} + e^{-E\,(N_t - t)}\right) \qquad (60)$$

in a range $t_1 \le t \le t_2$, so that the goodness of fit in the sense discussed for correlated data in [19] is acceptable. Our E_{k_1} correlations functions at $\lambda = 0.4$ and $\lambda = 0.9$ are shown in Fig. 6. The corresponding $m^2_{\rm photon}$ estimates are compiled in table III. The last column of the table gives the lowest non-zero lattice momentum squared.

While in [21] the photon mass estimates from simulations on $4^3 16$ lattices were within statistical errors consistent with zero, this is due to increased statistical accuracy no longer true, instead $m^2_{\rm photon}$ comes out negative. This holds not just for our action, but also for pure U(1) LGT, where we obtained $m^2_{\rm photon} = -0.2102\ (17)$ on a $4^3 16$ lattice at $\beta_a = 1.1$. Apparently we are dealing with an infrared cutoff effect, which disappears with increasing

TABLE III: Lattice sizes, statistics and photon mass estimates at $\lambda = \lambda_1 = 0.4$ and $\lambda = \lambda_2 = 0.9$.

Lattice	$n_{\rm es}$	$m^2_{\rm photon}(\lambda_1)$	$m^2_{\rm photon}(\lambda_2)$	$4\sin^2(k_1/2)$
$4^3 16$	2^{11}	$-0.252\ (20)$	$-0.289\ (21)$	2
$6^3 24$	2^{13}	$-0.080\ (11)$	$-0.0728\ (78)$	1
$8^3 32$	2^{14}	$-0.0138\ (18)$	$-0.0248\ (14)$	0.585786
$10^3 48$	2^{14}	$-0.0100\ (20)$	$-0.0123\ (11)$	0.381966
$12^3 64$	2^{14}	$-0.0034\ (12)$	$-0.0061\ (07)$	0.267949

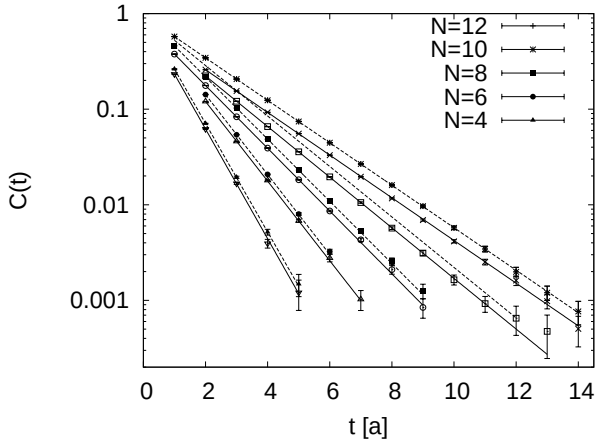

FIG. 6: Correlation functions data and fits for the photon mass estimates. The up-down order of the curves agrees with that of the labeling. The upper in a pair of curves is always at $\lambda = 0.9$ and the lower at $\lambda = 0.4$.

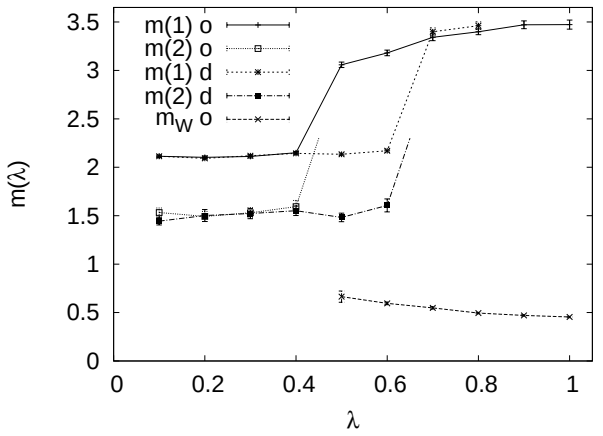

FIG. 7: Glueball and vector boson mass estimates on a $4^3 16$ lattice (o ordered and d disordered SU(2) starts).

lattice size and becomes thus consistent with [22] where $m^2_{\rm photon} = 0$ was again found within statistical errors for pure U(1) LGT. So, we conclude that $m^2_{\rm photon} \to 0$ for $N \to \infty$ holds also in our cases.

For an overview of the SU(2) glueball spectrum a $4^3 16$ lattice appears to be large enough, because glueball mass values turn out to be high. Compared to the E_{k_1} correlations, the signal from glueball correlation functions is very noisy, strongest for the lowest lying zero momentum A_1^{++} representation of the cubic group. In Fig. 7 we give for the A_1^{++} plaquette operator estimates $m(1)$ from correlations $0 \le t \le 1$ and $m(2)$ from $1 \le t \le 2$. In the disordered phase one has also signals for $t = 3$ which tend to give somewhat lower values than $m(2)$, but are so noisy that they overlap within statistical errors with $m(2)$. In the ordered phase signals are even weaker, so that the correlations at $t = 2$ include in most cases zero within two error bars. We give therefore only the $m(1)$ values, which lie considerably higher than in the disordered phase, with a hysteresis visible at the transition. One may conjecture that there are no glueball states in an eventual quantum continuum limit of the ordered phase. Instead, as shown next, with vanishing SU(2) string tension the glueball spectrum appears to break up into massive vector bosons.

Within Higgs model simulations on the lattice trial operators for the W mass are given by [23]

$$W_{i,\mu}(x) \;=\; -i\,{\rm Tr}\,[\tau_i\, W_\mu(x)]\;, \qquad (61)$$

where $W_\mu(x)$ is the gauge invariant link variable

$$W_\mu(x) \;=\; g^\dagger(x+\hat{\mu}a)\, V_\mu(x)\, g(x) \qquad (62)$$

and the SU(2) matrix $g(x)$ collects the angular variables of a complex doublet scalar field. This is also a gauge invariant operator for our action (21) with scalar fields. Our simulations correspond to this action at very large κ after fixing the gauge, so that (61) becomes

$$V_{i,\mu}(x) \;=\; -i\,{\rm Tr}\,[\tau_i\, V_\mu(x)]\;. \qquad (63)$$

TABLE IV: Effective 0^{++} glueball masses for $t = 1, 2$ and vector boson mass m_W.

	$\lambda = 0.4$		$\lambda = 0.9$		
Lat	$m(1)$	$m(2)$	$m(1)$	$m(2)$	m_W
$4^3 16$	2.144 (14)	1.551 (49)	3.471 (40)	noise	0.4706 (65)
$6^3 24$	2.0925 (46)	1.451 (23)	3.380 (21)	2.99 (32)	0.3385 (32)
$8^3 32$	2.1175 (37)	1.509 (18)	3.396 (16)	2.70 (26)	0.2901 (13)
$10^3 48$	2.1144 (38)	1.498 (13)	3.393 (12)	2.91 (24)	0.2729 (09)
$12^3 64$	2.1173 (32)	1.509 (12)	3.400 (12)	2.83 (20)	0.2677 (09)

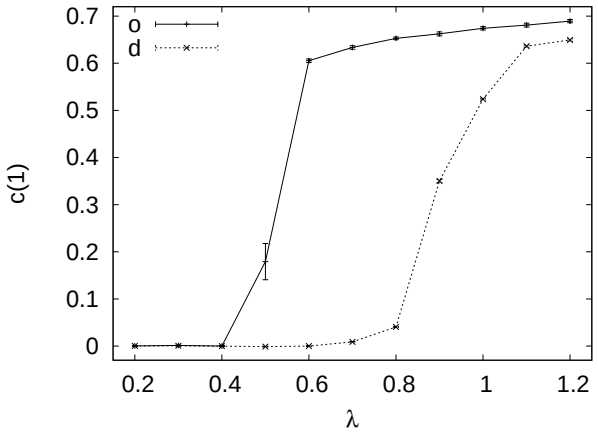

FIG. 8: Vector boson correlation function on a $4^3 16$ lattice at $t = 1$ (o ordered and d disordered SU(2) starts).

In the following we calculate vector boson masses from correlations of this operator.

In contrast to the zero momentum correlations of our glueball trial operators, those of $V_{i,\mu}$ turn out to be beautifully strong in the ordered phase, while they are zero in the disordered phase. For the $4^3 16$ lattice the hysteresis of the $t = 1$ correlation is shown in Fig. 8. At large λ values ($\lambda = 1.0$ and $\lambda = 1.2$) domain walls appear to prevent equilibration of disordered starts. Mass estimates in the ordered phase from cosh fits (60) are found in the lower right part of Fig. 7 (left of the transition m_W masses are infinite). As these masses rely on long range correlations finite size corrections are substantial. For several lattice sizes m_W estimates at $\lambda = 0.9$ are collected in table IV, where we also see that there are almost no finite size effects for glueball masses.

The correlation function for the m_W fit at $\lambda = 0.9$ on our largest lattice is depicted in Fig. 9. The signal can be followed up to more than 20 lattice spacings in the N_t extension. While significant for small volumes, finite size corrections decrease quickly for larger volumes. For our $N \ge 8$ lattices a fit of the form $m_W(N) = m_W + const/N^3$ works well and is depicted in Fig. 10. It yields the infinite volume extrapolation $m_W = 0.2567\,(10)$ with $Q = 0.22$ goodness of fit.

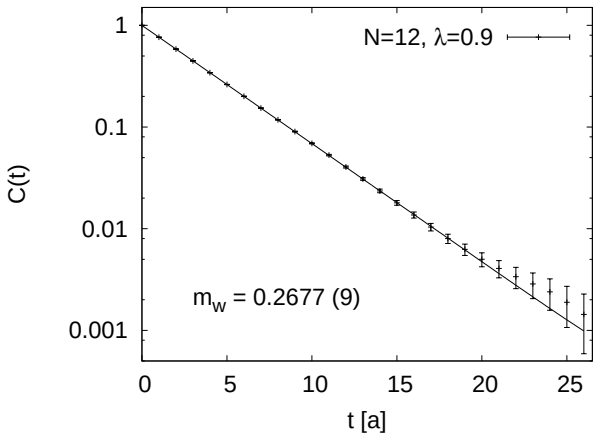

FIG. 9: Correlation function data and fit for m_W mass on a $12^3 64$ lattice.

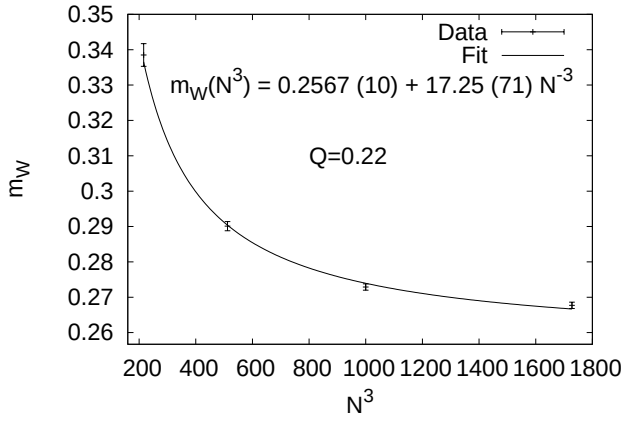

FIG. 10: Finite size extrapolation of the W mass.

IV. SUMMARY, OUTLOOK AND CONCLUSIONS

We have introduced a model of SU(2) and U(1) vector fields, which can be obtained from the gauge invariant interaction (21) between a scalar matrix field and the vector fields in the London limit $(\Phi^\dagger\Phi)^2 \to \tau_0$ (τ_0 2×2 unit matrix), i.e., $\kappa \to \infty$ in Eq. (21). On a finite lattice this interaction is for sufficiently large κ supposed to be indistinguishable from the $\kappa \to \infty$ limit. MC simulations of the quantum field theory on the lattice exhibits a phase transition between a deconfined phase with a glueball spectrum and a deconfined phase with a massive vector boson triplet. A massless photon is found in the spectrum of both phases.

Whether this quantum field theory just lives on the lattice or has a quantum continuum limit remains to be clarified. The question of its renormalizability requires perturbative investigations, which are beyond the scope of this paper. Due to the London limit the scalar field becomes that of a non-linear σ model, which is usually non-renormalizable. However, our situation is peculiar, because the scalar field can be absorbed into extended gauge transformations of the SU(2) and U(1) vector fields (17), (18) and the theory we are interested in is the one without scalar fields as first formulated in [9].

In itself the lattice properties are rather remarkable, most of all the evidence from Fig. 8 to 10 for a massive vector boson triplet in the deconfined, but not in the confined, phase.

Acknowledgments

This work was in part supported by the DOE grant DE-FG02-97ER41022 and by a Research Award of the Humboldt Foundation. Part of the work was done at Leipzig University and I am indebted to Wolfhard Janke and his group for their kind hospitality. Further, I thank Holger Perlt and Arwed Schiller for useful discussions. Some of the computer programs used rely on collaborations with Alexei Bazavov and benefited from programing help by Hao Wu.

Appendix A: Invariance under Extended Gauge Transformations.

Following [10] we show the invariance of (27) under extended gauge transformations. Expanding a calculation of [1] slightly, we find

$$\begin{aligned} & g_a\partial_\mu A'_\nu - g_b\partial_\nu B'_\mu = \\ & \partial_\mu[G g_a A_\nu G^{-1} + i(\partial_\nu G)G^{-1}] \\ - \; & \partial_\nu[G g_b B_\mu G^{-1} + i(\partial_\mu G)G^{-1}] = \end{aligned} \tag{A1}$$

$$\begin{aligned} & G(g_a\partial_\mu A_\nu - g_b\partial_\nu B_\mu)G^{-1} \\ + \; & [(\partial_\mu G)g_a A_\nu - (\partial_\nu G)g_b B_\mu]G^{-1} \\ + \; & G[g_a A_\nu(\partial_\mu G^{-1}) - g_b B_\mu(\partial_\nu G^{-1})] \\ + \; & i\,[(\partial_\nu G)(\partial_\mu G^{-1}) - (\partial_\mu G)(\partial_\nu G^{-1})] \end{aligned} \tag{A2}$$

Using $(\partial_\mu G^{-1})G + G^{-1}(\partial_\mu G) = \partial_\mu(G^{-1}G) = 0$, this can be transformed to

$$\begin{aligned} & g_a\partial_\mu A'_\nu - g_b\partial_\nu B'_\mu = \\ & G\,(g_a\partial_\mu A_\nu - g_b\partial_\nu B_\mu)\,G^{-1} \\ + \; & G\left\{\left[G^{-1}(\partial_\mu G), g_a A_\nu\right] - \left[G^{-1}(\partial_\nu G), g_b B_\mu\right]\right\} G^{-1} \\ - \; & i\,G[(\partial_\mu G^{-1})(\partial_\nu G) - (\partial_\nu G^{-1})(\partial_\mu G)]G^{-1}\,. \end{aligned} \tag{A3}$$

The commutator term transforms as

$$\begin{aligned} & i\,g_a g_b\,[B'_\mu, A'_\nu] = \\ & i\,g_a g_b\,[(G B_\mu G^{-1} + (i/g_b)(\partial_\mu G)G^{-1}), \\ & \qquad (G A_\nu G^{-1} + (i/g_a)(\partial_\nu G)G^{-1})] \end{aligned} \tag{A4}$$

$$
\begin{aligned}
&= i\, g_a g_b G[B_\mu, A_\nu] G^{-1} \qquad \text{(A5)}\\
&- G\{[G^{-1}(\partial_\mu G), g_a A_\nu] - [G^{-1}(\partial_\nu G), g_b B_\mu]\} G^{-1}\\
&+ i\, G[(\partial_\mu G^{-1})(\partial_\nu G) - (\partial_\nu G^{-1})(\partial_\mu G)] G^{-1}\,.
\end{aligned}
$$

Combining (A3) and (A5) yields (46).

Appendix B: Classical continuum limit of the action with scalar fields.

We write the scalar matrix field of the action (21) as

$$\Phi(x) \;=\; \phi_1(x)\,\phi_2(x) \qquad \text{(B1)}$$

with ϕ_1 and ϕ_2 defined by (47) and factor (21) into the form

$$
\begin{aligned}
S^s_{\mu\nu} \;&=\; \frac{\lambda^s}{4}\,\mathrm{Re\,Tr}\,(S_{1\mu\nu})\;\mathrm{Tr}\,(S_{2\mu\nu}) + h.c.\\
&+\; \kappa\,\mathrm{Tr}\,[(\Phi^\dagger\Phi - \tau_0)^2]\,. \qquad \text{(B2)}
\end{aligned}
$$

As calculation of the classical continuum limit of this action leads to tedious algebra, we rely on the algebraic program FORM [24]. For this it is convenient to write (B2) in a symmetric form with the position x at the center of the plaquette:

$$
\begin{aligned}
&S_{1\mu\nu} = \qquad \text{(B3)}\\
&\left[\phi_1^\dagger\left(x - \hat\mu\frac{a}{a} - \hat\nu\frac{a}{2}\right)\,U_\mu\left(x - \hat\nu\frac{a}{2}\right)\,\phi_1\left(x + \hat\mu\frac{a}{2} - \hat\nu\frac{a}{2}\right)\right]\\
&\left[\phi_1^\dagger\left(x - \hat\mu\frac{a}{2} + \hat\nu\frac{a}{2}\right)\,U_\mu\left(x + \hat\nu\frac{a}{2}\right)\,\phi_1\left(x + \hat\mu\frac{a}{2} + \hat\nu\frac{a}{2}\right)\right]^\dagger,\\
&S_{2\mu\nu} = \qquad \text{(B4)}\\
&\left[\phi_2^\dagger\left(x + \hat\mu\frac{a}{2} - \hat\nu\frac{a}{2}\right)\,V_\nu\left(x + \hat\mu\frac{a}{2}\right)\,\phi_2\left(x + \hat\mu\frac{a}{2} + \hat\nu\frac{a}{2}\right)\right]\\
&\left[\phi_2^\dagger\left(x - \hat\mu\frac{a}{2} - \hat\nu\frac{a}{2}\right)\,V_\nu\left(x - \hat\mu\frac{a}{2}\right)\,\phi_2\left(x - \hat\mu\frac{a}{2} + \hat\nu\frac{a}{2}\right)\right]^\dagger.
\end{aligned}
$$

We expand the scalar fields ϕ_i, $i = 1, 2$, to order a^2. With ϵ and η of order a:

$$
\begin{aligned}
\phi_i(x + \epsilon\hat\mu + \eta\hat\nu) \;&=\; \phi_i(x) + \epsilon\partial_\mu\phi_i(x) + \eta\partial_\nu\phi_i(x)\\
&+\; \eta\epsilon\partial_\nu\partial_\mu\phi_i(x) + \dots\,. \qquad \text{(B5)}
\end{aligned}
$$

The gauge matrices defined by (7) have to be expanded up to order a^4 in the lattice spacing. For the gauge potential the substitutions

$$A_\mu\,(x + \eta\hat\nu) \;=\; A_\mu(x) + \eta\partial_\nu A_\mu(x)\,, \qquad \text{(B6)}$$

$$B_\nu\,(x + \epsilon\hat\mu) \;=\; B_\nu(x) + \epsilon\partial_\mu B_\nu(x)\,, \qquad \text{(B7)}$$

are done. These expansions generate more terms (the computer does not care) than the analogue expansions of (21), but avoid some complications in the identification of covariant operators. We write now for $i = 1, 2$

$$S_{i\mu\nu} = \left(\phi_i^\dagger\phi_i\right)^2 + a^2\,S_{i\mu\nu}(2) + a^4\,S_i(4) + \dots\,. \qquad \text{(B8)}$$

The traces of the order a and a^3 terms of this expansion are seen to vanish. The covariant contribution of

$$\mathrm{Re\,Tr}\;[S_{1\mu\nu}(2)]\;\mathrm{Tr}\;[S_{2\mu\nu}(2)] \qquad \text{(B9)}$$

to (B2) comes from the anti-Hermitean terms

$$
\begin{aligned}
&\mathrm{Tr}\;[S_{2\mu\nu}(2)] = \frac{1}{4}\,\mathrm{Tr}\,\Big\{\left(D^b_\nu\,\phi_2\right)^\dagger\phi_2\;\left(D^b_\mu\,\phi_2\right)^\dagger\phi_2\\
&+\left(D^b_\nu\,\phi_2\right)^\dagger\phi_2\;\phi_2^\dagger\,D^b_\mu\,\phi_2 + \left(D^b_\mu\,\phi_2\right)^\dagger\phi_2\;\left(D^b_\nu\,\phi_2\right)^\dagger\phi_2\\
&-\left(D^b_\mu\,\phi_2\right)^\dagger\phi_2\;\phi_2^\dagger\,D^b_\nu\,\phi_2 - \phi_2^\dagger\,D^b_\nu\,\phi_2\;\left(D^b_\mu\,\phi_2\right)^\dagger\phi_2\\
&-\phi_2^\dagger\,D^b_\nu\,\phi_2\,\phi_2^\dagger\,D^b_\mu\,\phi_2 + \phi_2^\dagger\,D^b_\mu\,\phi_2\;\left(D^b_\nu\,\phi_2\right)^\dagger\phi_2\\
&-\phi_2^\dagger\,D^b_\mu\,\phi_2\,\phi_2^\dagger\,D^b_\nu\,\phi_2 - 2\,\phi_2^\dagger\,\phi_2\;\left(D^b_\nu\,\phi_2\right)^\dagger D^b_\mu\,\phi_2\\
&-2\,\phi_2^\dagger\,\phi_2\;\left(D^b_\mu\,D^b_\nu\,\phi_2\right)^\dagger\;\phi_2 + 2\,\phi_2^\dagger\,\phi_2\;\left(D^b_\mu\,\phi_2\right)^\dagger D^b_\nu\,\phi_2\\
&+2\,\phi_2^\dagger\,\phi_2\,\phi_2^\dagger D^b_\mu\,D^b_\nu\,\phi_2\Big\} \qquad \text{(B10)}
\end{aligned}
$$

and $\mathrm{Tr}\;[S_{1\mu\nu}(2)]$, which is obtained by interchanging A_α with B_α (D^a_α with D^b_α) and then the subscripts μ and ν.

In the London limit $\mathrm{Tr}\;[S_{1\mu\nu}(2)]\;\mathrm{Tr}\;[S_{2\mu\nu}(2)]$ gives the contribution $\sim \mathrm{Tr}\;(\partial_\nu A_\mu\,\partial_\mu B_\nu)$ to the action (27). The terms $\sim \mathrm{Tr}\;(\partial_\nu A_\mu\,\partial_\nu A_\mu)$ and $\sim \mathrm{Tr}\;(\partial_\mu B_\nu\,\partial_\mu B_\nu)$ of (27) come from the $a^4\,(\phi_1^\dagger\,\phi_1)^2\,S_{2\mu\nu}(4)$ and $a^4\,S_{1\mu\nu}(4)\,(\phi_2^\dagger\,\phi_2)^2$ contributions to (B2), whose calculation we found too tedious to pursue. For small oscillations about the expectation value of the scalar fields

$$S_{1\mu\nu}(4) = S_{1\mu\nu}(2)^2 \;\;\text{and}\;\; S_{2\mu\nu}(4) = S_{2\mu\nu}(2)^2 \qquad \text{(B11)}$$

are good approximations, illustrating the typical gauge invariant terms encountered.

[1] C. Quigg, *Gauge Theories of the Strong, Weak, and Electromagnetic Interactions*, Addison-Wesley, 1983.

[2] S. Weinberg, Phys. Rev. Lett. **19**, 1264 (1967); A. Salam, Proceedings of the 8th Nobel Symposium, N. Svartholm (editor), Almqvist and Wiksell, Stockholm 1968.

[3] No useful correlations beyond one lattice spacing were found for spin 1, indicating a high mass: K. Ishikawa, G. Schierholz and M. Teper, Z. Phys. C **19**, 327 (1983). Subsequent improvements focused on spin 0 and 2: C. Michael and M. Teper, Phys. Lett. B **199**, 95 (1987).

[4] C.B. Lang, C. Rebbi, and M. Virasoro, Phys. Lett. B **104**, 294 (1981); H. Kühnelt, C.B. Lang, and G. Vones, Nucl. Phys. B **230** [FS10], 16 (1984); M. Tomiya and T. Hattori, Phys. Lett. B **140**, 370 (1984); I. Montvay, Phys. Lett. B **150**, 441 (1985); W. Langguth and I. Montvay, Phys. Lett. B **165**, 135 (1985).

[5] K. Wilson, Phys. Rev. D **10**, 2445 (1974).

[6] A.H. Guth, Phys. Rev. D **21**, 2291 (1980).

[7] First pointed out by a PRD referee.

[8] F. London and H. London, Physica **2**, 341 (1935).

[9] B.A. Berg, arXiv:0909.3340. MC results reported in this reference suffer from a bug in the simulation program. This accounts for the difference between some of the figures here and corresponding ones of this reference.

[10] B.A. Berg, arXiv:0910.4742.

[11] I. Montvay and G. Münster, *Quantum Fields on a Lattice*, Cambridge University Press, 1994.

[12] H.J. Rothe, *Lattice Gauge Theories*, World Scientific, 2005.

[13] C. Roiesnel, hep-lat/9509092 and references therein.

[14] R. Shrock, Nucl. Phys. B **267**, 301 (1986).

[15] Compare chapter 6.1.1 of [11] (κ and λ are interchanged with respect to their notation).

[16] J. Jersak, T. Neuhaus, and P.M. Zerwas, Phys. Lett. B **133**, 103 (1983).

[17] A. Hurwitz, Nachr. Gött. Ges. Wissensch. (1897) p.71; A. Haar, Ann. Math. **34**, 147 (1933).

[18] A. Bazavov and B.A. Berg, Phys. Rev. D **71**, 114506 (2005); A. Bazavov, B.A. Berg, and U.M. Heller Phys. Rev. D **72** 117501 (2005).

[19] B.A. Berg, *Markov Chain Monte Carlo Simulations and Their Statistical Analysis*, World Scientific, 2004.

[20] M. Creutz, Phys. Rev. D **21**, 2308 (1980).

[21] B.A. Berg and C. Panagiotakopoulos, Phys. Rev. Lett. **52**, 94 (1984).

[22] P. Majumdar, Y. Koma, and M. Koma, Nucl. Phys. B **677**, 273 (2004).

[23] Eq. (6.27) of [11] (their V is our W and our V their U).

[24] J.A.M. Vermaseren, M. Tentyukov and J. Vollinga, Reference manual for FORM, `www.nikhef.nl/~form` .